NBS
PUBLICATIONS

NBSIR 85-3112

Development of Power System Measurements -- Quarterly Report April 1, 1984 to June 30, 1984

R. E. Hebner, Editor

NBSIR 85-3112

DEVELOPMENT OF POWER SYSTEM MEASUREMENTS -- QUARTERLY REPORT APRIL 1, 1984 TO JUNE 30, 1984

R. E. Hebner, Editor

U.S. DEPARTMENT OF COMMERCE
National Bureau of Standards
Center for Electronics and Electrical Engineering
Electrosystems Division
Gaithersburg, MD 20899

July 1984

Issued March 1985

U.S. DEPARTMENT OF COMMERCE, Malcolm Baldrige, *Secretary*

NATIONAL BUREAU OF STANDARDS, Ernest Ambler, *Director*

Foreword

This report summarizes the progress on three technical investigations during the third quarter of FY 84. Although reasonable efforts have been made to ensure the reliability of the data presented, it must be emphasized that this is an interim report so that further experimentation and analysis may be performed before the conclusions from any of these investigations are formally published. It is therefore possible that some of the observations presented in this report will be modified, expanded, or clarified by our subsequent research.

TABLE OF CONTENTS

LIST OF FIGURES

LIST OF TABLES

DEVELOPMENT OF POWER SYSTEM MEASUREMENTS -- QUARTERLY REPORT
April 1, 1984 to June 30, 1984

R. E. Hebner, Editor

This report documents the progress of three technical
investigations sponsored by the Department of Energy and performed by
or under a grant from the Electrosystems Division, the National Bureau
of Standards. The work described covers the period April 1, 1984 to
June 30, 1984. This report emphasizes the errors associated with
measurements of dc electric fields, the properties of corona in
compressed SF_6 gas, and the measurement of voltage pulses on
nanosecond time scales.

Key words: deconvolution; electric fields; gaseous insulation;
partial discharges; pulsed voltage measurement; SF_6; solid insulation.

1. INTRODUCTION

Under an interagency agreement between the U.S. Department of Energy and
the National Bureau of Standards, the Electrosystems Division, NBS, has been
providing technical support for DOE's research on electric energy systems. This
support has concentrated on the measurement of electric and magnetic fields, the
measurement of interfacial phenomena, and of partial discharge phenomena, and
the measurement of voltage and current on nanosecond time scales. The technical
progress made during the quarter April 1, 1984 to June 30, 1984 is summarized in
this report.

2. ELECTRIC AND MAGNETIC FIELD MEASUREMENTS
Subtask Nos. 01 and 02

The objectives of this investigation are to develop methods to evaluate and
calibrate instruments which are used, or are being developed, to measure the
electric field, the space charge density, and current density in the vicinity of
high-voltage dc transmission lines and in apparatus designed to simulate the
transmission line environment; to provide electrical measurement support for
DOE-funded efforts to determine the effects of ac fields on biological systems,
and to provide similar support for biological studies which will be funded by
the State of New York.

During the current reporting period, an improved model was developed for
fluid flow through an opening in a plane. The present calculation is three-
dimensional in nature and provides better agreement with air speed measurement
results than an earlier two-dimensional analysis. The calculations are relevant
to predicting perturbations of ion motion near the aperture of aspirator-type
ion counter operating in the ground plane. A knowledge of how rapidly such a
perturbation becomes negligible provides guidance as to the accuracy with which
the NBS-developed parallel plate facility can provide a constant ion density and
thus can serve as a standard ion source.

2.1 Flow Induced By a Draft Down a Hole

An aspirator type ion counter, operated in the ground plane, extracts air
from the high field side of the ground plane. This fluid (air) flow can perturb

the ion distribution. This perturbation, while it may be less important for measurement near dc transmission lines, may be significant in biological exposure facilities and in laboratory calibration systems.

A distribution of point sinks is used to model the three-dimensional, steady air flow which is induced in a half-space by a known outflow across the boundary. In a rotationally symmetric case, velocities are found analytically. In the general case, numerical integration may be applied to approximate the flow.

Air is drawn into an opening in a broad flat surface at a speed much below that of sound. To determine the flow above the surface, the flow is modeled as steady, irrotational, and incompressible in the upper half-space consisting of points $x = (x_1, x_2, x_3)$ such that $x > 0$. We wish to find the velocity, u, satisfying the boundary conditions for x in the boundary ($x_3 = 0$):

$$u_n(\vec{x}) = u_o \text{ for } \vec{x} \text{ in } \Omega \tag{1a}$$

$$u_n(\vec{x}) = 0 \text{ for } \vec{x} \text{ not in } \Omega \tag{1b}$$

Here, u_n is the component of $\vec{u}$ normal to the boundary and Ω is the opening, an open, bounded set of points in the boundary. We also require the velocity at infinity to be zero:

$$\lim_{|x| \to \infty} |\vec{u}(\vec{x})| = 0 \tag{1c}$$

Thus, in the plane $x_3 = 0$, we have the situation shown in figure 1.

The central idea is to represent the flow field as a linear superposition of point sinks over the region Ω [1]. It emerges from our analysis that the boundary conditions are satisfied and that for one simple, but important region, Ω, the velocity can be found analytically.

The continuity equation for incompressible flow is

$$\vec{\nabla} \cdot \vec{u} = 0. \tag{2}$$

Irrotationality is given by $\vec{\nabla} \times \vec{u} = 0$. The solution for a point sink at $\vec{x}'$ with volume flux m is [2]

$$\vec{u}(\vec{x}) = \frac{m}{4\pi} \frac{\vec{x} - \vec{x}'}{|\vec{x} - \vec{x}'|^3} \tag{3}$$

The superposition of point sinks of constant strength which are uniformly distributed over the region Ω, gives rise to the velocity field:

$$\vec{u}(\vec{x}) = \int\int_\Omega \frac{u_o}{4\pi} \frac{\vec{x} - \vec{x}'}{|\vec{x} - \vec{x}'|^3} dx'_1 dx'_2 , \tag{4}$$

where m and u_o are related by $m = 2u_o \cdot \text{area}(\Omega)$ and m is the volume flux into the sink Ω from both the upper and lower half spaces. In the case that the flux comes from the upper half only, one must replace the constant
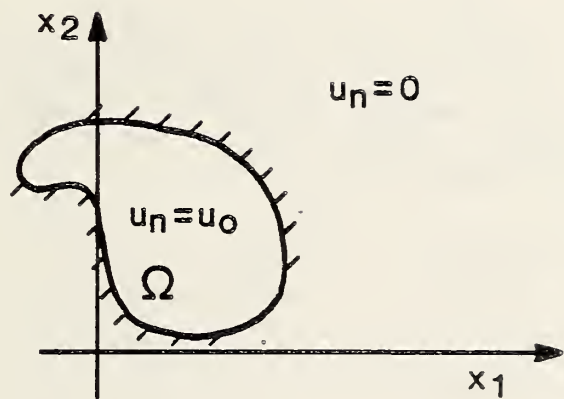
Figure 1. The boundary conditions.

3

$$\frac{u_0}{4\pi} \quad \text{by} \quad \frac{u_0}{2\pi} \; . \tag{5}$$

In the interior of the flow, for $\vec{x}$ in the proper half space $x_3 > 0$, the integrand in (4) is absolutely integrable and one may differentiate through the integral to establish that $\vec{u}$ satisfies the differential equation (2).

Some care must be taken in establishing the boundary conditions (1). When $\vec{x}$ lies outside Ω but in the plane $x_3 = 0$, the vector $\vec{x}-\vec{x}'$, which appears in the integrand, has a zero component in the normal direction. The integral converges and so $\vec{u}(\vec{x})$ is defined and has a normal component of zero, i.e.,

$$u_n(\vec{x}) = 0 \; . \tag{6}$$

For $\vec{x}$ in Ω, the integrand in (4) has a singularity at $\vec{x}' = \vec{x}$ and is not summable. Consider, however, the velocity at a small distance, d, above the point $\vec{x} = (x_1, x_2, 0)$. At $\vec{x}_d = (x_1, x_2, d)$, the velocity can be estimated and

$$\lim_{d \to 0} u_n(\vec{x}_d) = u_0. \tag{7}$$

To show this, consider a disk centered at $\vec{x}$ and lying entirely in Ω. Let the disk radius be R as shown in figure 2, and let $r = |\vec{x}'-\vec{x}|$. Integrating separately over the disk and its complement in Ω, and converting to polar coordinates for the disk, one sees that at x_d, $d \ll R$, the normal component of the velocity is well estimated by

$$U_n = \frac{u_0}{2\pi} \int_0^{2\pi} \int_0^R \frac{d}{(r^2+d^2)^{3/2}} \, r\,dr\,d\theta \tag{8}$$

$$= u_0 \left\{ 1 - \frac{d}{(R^2+d^2)^{1/2}} \right\} \; . \tag{9}$$

As $d \to 0$, we get $u_n \to u_0$, which was to be shown.

Note that when Ω is a disk, the velocity along the central axis, $x_1 = x_2 = 0$, is given by eq (9). Thus for a circular hole

$$\vec{u}(0,0,x_3) = (0,0,u_0(1 - \alpha(1+\alpha^2)^{-1/2})), \quad \alpha = \frac{x_3}{R} \; . \tag{10}$$

The validity of this model has been verified with measurements made along the central axis (see below). For a more complicated Ω, the evaluation of $\vec{u}(x)$ may require a quadrature. Geometric complexity is of no difficulty as long as Ω can be decomposed into triangles and disks. In this case computer software is available for the necessary calculations.

For application of this method to flows in a half space, the velocities away from the boundary are accurately determined. Neglecting viscosity gives good results because there are no upstream boundaries and consequently no sources of vorticity in the far field. The procedure runs into difficulty at
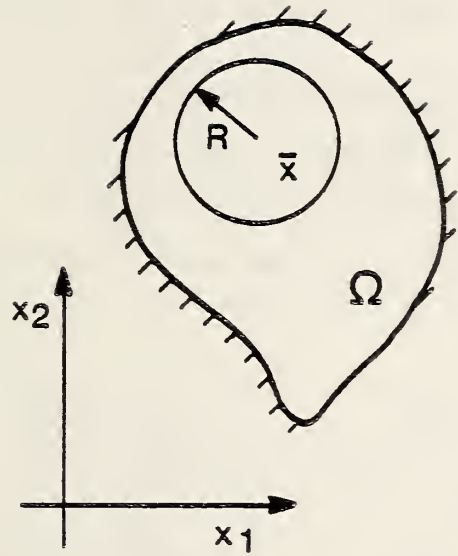
Figure 2. Estimating u_n near Ω.

the edge of the region Ω where the velocity given by this method is infinite. This non-physical solution is the result of neglecting the boundary layer. In the apparatus under consideration, the Reynolds number ranges from 5000 to 30000. For such values, a more accurate determination of flow field in the upstream region is possible, because, for slightly viscous flow, a jet issues on the downstream side of the hole. One must characterize the jet and use it to determine the velocity, u_n, at the hole. Then eq (10) may be used to find the upstream flow more accurately.

The central velocities given by eq (10) agree with experiment. Measurements of velocities are made along the central axis lying over a rectangular opening. The data is used to fit the model eq (10) for a circular opening. Table 1 shows the results of experiment and theory. The measurements are made at different flow rates through the same opening and all figures are normalized so $u(0.5 \text{ cm}) = 1$. Two techniques are used to find an effective R and the corresponding u_0. In case 1, two measurements (d, u(d)) yield two simultaneous equations in u_0 and R. These are solved iteratively to find the model parameters. In case 2, one selects R so that πR^2 is equal to the known area of the opening and u_0 is chosen so that $u(0.5 \text{ cm}) = 1$. Figure 3 displays the measurements and the theoretical curve of case 2.

Table 1. A comparison of theory to experiment for normalized air speed into a small opening (5.1 cm x 5.1 cm), $u(0.5 \text{ cm}) = 1$.

	Measurement				Theory			
	1(▲)	2(•)	3(■)		Case 1			Case 2
R					3.19	2.98	2.91	2.88 cm
d					▲	■	▲	
0.0**	Not Measured				1.18	1.20	1.26	1.21
0.5	1.0	1.0	1.0		1.00*	1.00*	1.04	1.00*
1.5	.68	.72	.66		.68*	.66*	.68*	.65
3.5	.29	.27	.25		.31	.29	.29*	.27
5.5	.13	.14	.12		.16	.14	.15	.14
7.5	.08	.08	.10		.09	.09	.09	.08

* Agreement is an artifact of data fitting
**No measurements made, theory gives u_0.

Uncertainties in the air speed measurements range from 5% for the highest values, to 10% for the lowest values. The position of the probe is known to within ~1 mm. Assuming the model calculation to be correct, a linear error analysis shows that the uncertainty in u_0 is <10%.

We have presented an analytic form of the flow induced by a draft through a hole in a flat boundary. The model is fully three-dimensional and provides a closed form for the velocity in a problem of interest; i.e., for an aspiration-type ion counter operated in the ground plane. Some work is needed to implement this method on the computer. It is interesting to note that in the evaluation of eq (4) by quadrature, the boundary condition, eq (1a), can be generalized to allow $u_n(x)$ to vary over the opening. The inclusion of the boundary layer in the model would extend its usefulness to the edge of the half-space, but the influence of this boundary layer at the ground plane is probably not important for the description of the perturbations introduced by the ion counter.
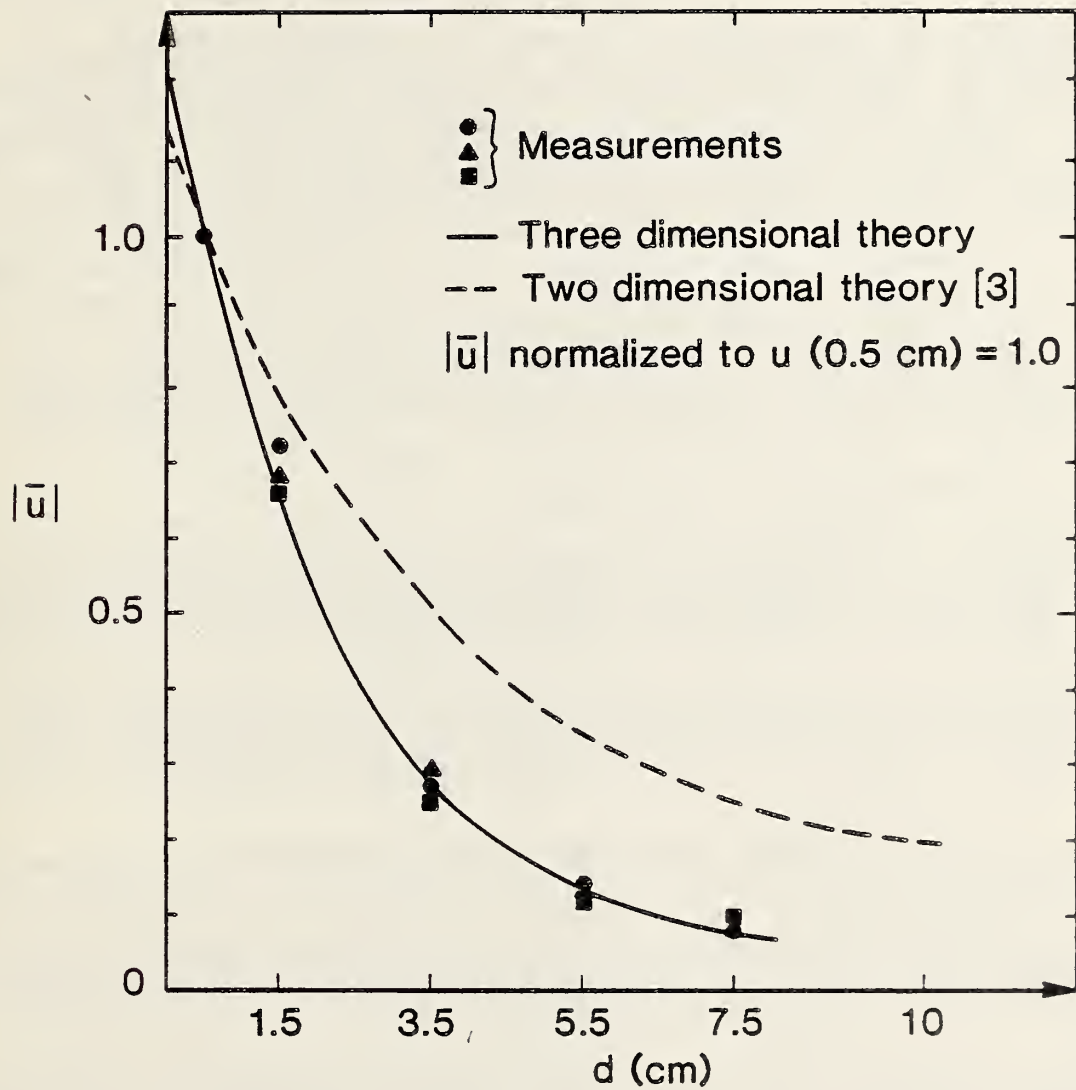
Figure 3. Air speed versus height (non-dimensional $|u|$). The measured values were obtained using three flow rates through the opening, 0.37×10^{-2} m^3/s (■), 0.69×10^{-2} m^3/s (●), and 1.7×10^{-2} m^3/s (▲). The data have been normalized to unity at d = 0.5 cm.

During the next quarter, a measurement system for characterization of ambient ac magnetic fields will be developed. Electrical measurements associated with the operation of an ion counter operating in the ground plane will be performed under a test line and in the NBS parallel plate apparatus.

For further information contact Dr. M. Misakian at (301) 921-3121.

3. TECHNICAL ASSISTANCE FOR FUTURE INSULATION SYSTEMS RESEARCH
Subtask No. 03

The objective of this project is to develop diagnostic techniques to monitor, identify, and predict degradation in future compressed gas electrical insulating systems under normal operating conditions. The focus is on the fundamental information and data needed to improve test design and performance evaluation criteria. The scope of the project encompasses the following investigations: 1) measurement and calculation of electric discharge inception in compressed electronegative gases; 2) measurement, calculation, and compilation of fundamental data on electron transport and electrical breakdown in gases; 3) measurement of absolute electric discharge-induced decomposition rates in gaseous dielectrics; and 4) examination of the influence of contaminants like water vapor on the performance of compressed gas-insulated systems. Emphasis is given in these investigations to the development and evaluation of new measurement techniques.

The planned activities for FY84 include:

1) Preparation of conference and archival papers presenting results of our measurements on the production rates for the oxyfluorides SOF_2, SO_2F_2 and SOF_4, and SO_2 and H_2O generated by corona discharges in SF_6 or SF_6/H_2O mixtures;

2) Extension of the measurements on by-product production rates in gas discharges to the mixtures, $SF_6 + O_2$, $SF_6 + N_2$, $SF_6 + CO_2$, and $SF_6 + c-C_4F_8 + CHF_3$;

3) Compilation of a computerized bibliography of electrical breakdown data in insulating gases and publication of this bibliography in an NBS report;

4) Investigation of the effects of trace quantities of water vapor on the enhancement of electron avalanche growth and corona discharge development in SF_6.

The bibliography mentioned in activity 3 has been completed and is available as an NBS Technical Note [4]. The bibliography contains 1) a list of archival papers and books that present data on electrical breakdown in gases and which have been published since 1950; 2) a computer generated index indicating the references that give particular types of data for each gas; 3) an author index; and 4) a list of relevant technical conferences.

The citations given in the bibliography contain experimental or theoretical data on breakdown which include: 1) sparking potentials; 2) breakdown voltages; 3) critical fields, or field-to-gas density ratios; 4) corona inception voltages; 5) voltage-time characteristics; 6) relative and absolute dielectric strengths; and 7) breakdown probabilities. The types of data which were

considered include those which apply to: 1) uniform and nonuniform electric fields; 2) ac, dc, and impulse voltages; and 3) possible special effects associated with particles, surfaces, interfaces, and corona. The bibliography is intended to serve as a guide in locating data on breakdown which are most relevant to particular applications. All gases likely to be encountered in electrical insulation applications are included. Any omissions are due either to a failure to locate relevant references or to a complete lack of data. Copies of the bibliography are available from the National Bureau of Standards, Electrosystems Division, Gaithersburg, MD 20899, and from the U. S. Government Printing Office, Washington, DC 20402.

The emphasis of our effort during the past quarter was on activity 1. An analysis of all previously acquired data on SOF_4 production in SF_6 corona discharges was carried out to determine the absolute production rates for this species. New procedures for minimizing errors associated with GC/MS column and ion source conditioning effects in quantitative analysis of gases were developed to improve the accuracy and reliability of measurements on discharge-generated gas species production rates.

The conference paper entitled "Production Rates for Discharge Generated SOF_2, SO_2F_2, and SO_2 in SF_6 and SF_6/H_2O Mixtures" by R. J. Van Brunt, T. C. Lazo, and W. E. Anderson has been published in the Proceedings of the Fourth International Symposium on Gaseous Dielectrics, Knoxville, Tennessee, April - May, 1984 [5]. This paper presents the results of our measurements of the absolute production rates for SOF_2, SO_2F_2, SO_2, and H_2O generated by point-plane corona discharges under a wide range of conditions in SF_6 containing trace levels of water vapor. An archival paper describing all of the results on production of stable, oxygenated, gaseous species from corona discharges in SF_6 as well as giving detailed information about the analytical techniques employed has been prepared and is undergoing review. A discussion of the results presented in this paper is highlighted in this report. This includes discussion of a proposed mechanism for SF_6 decomposition in corona discharges that is consistent with previous observations of electrical, thermal, and laser-induced decomposition of SF_6 and SF_6/O_2 mixtures.

3.1 Results for Oxyfluoride Yields from SF_6 Corona

The most abundant, long-lived, stable, gaseous species generated by corona discharges in SF_6 gas containing trace levels of O_2 and H_2O are the oxyfluorides SOF_2, SOF_2F_2, and SOF_4. Results for the limiting constant production rates of SOF_2, SO_2F_2, and SOF_4 from corona are given in tables 2-4. Both the energy rates-of-production, r_u, and the charge rates-of-production, r_q, are listed as functions of discharge conditions (polarity, current, and power) and gas pressure. Gas pressures range from 114 kPa (~1.1 atm) to 300 kPa (~3 atm). Discharge currents from 1.5 µA to 64 µA with corresponding power dissipations from 0.054 W to 4.3 W are included. The limiting constant production rates were derived from linear least squares fits to the measured concentrations C versus either net energy dissipated, u, or net charge transported in the discharge, Q, for $u > u_{min}$ and $Q > Q_{min}$, where u_{min} and Q_{min} are the lowest values for which the assumptions of linearity hold [5].

Production rates were estimated in some cases for observable minor species, namely SO_2, OCS, and CO_2 as indicated in table 5. The rates for these are seen to be an order of magnitude or more smaller than those for the predominant oxyfluorides.

Table 2. Limiting values for SOF_2 production rates.

Polarity	Discharge Power (W)	Discharge Current (μA)	Gas Pressure (kPa)	Production Rates	
				(n moles/J)	(μ moles/C)
Pos.	0.804	20.0	116	1.28	49.5
	0.054	1.5	200	5.20	181
	0.335	8.0	200	4.69	195
	0.777	16.0	200	3.80	180
	0.198	4.0	300	4.06	187
	0.430	8.0	300	3.09	178
	0.945	16.0	300	2.64	172
Neg.	0.898	25.0	114	1.21	45.0
	0.230	8.0	200	1.52	35.2
	0.586	16.0	200	0.93	34.7
	0.821	20.0	200	0.68	34.1
	2.225	40.0	200	0.54	32.4
	4.290	64.0	200	0.44	33.7
	0.764	16.0	300	0.73	31.2
	1.140	21.0	300	0.41	23.9
	1.820	30.0	300	0.33	22.3

Table 3. Limiting values for SO_2F_2 production rates.

Polarity	Discharge Power (W)	Discharge Current (μA)	Gas Pressure (kPa)	Production Rates	
				(n moles/J)	(μ moles/C)
Pos.	0.804	20.0	116	1.83	69.7
	0.054	1.5	200	4.51	151
	0.154	4.0	200	4.07	158
	0.335	8.0	200	3.27	147
	0.777	16.0	200	2.10	109
	0.198	4.0	300	2.32	119
	0.430	8.0	300	2.03	113
	0.945	16.0	300	1.29	111
Neg.	0.898	25.0	114	0.52	18.0
	0.230	8.0	200	0.62	16.0
	0.586	16.0	200	0.47	16.9
	0.821	20.0	200	0.36	14.8
	2.215	40.0	200	0.25	13.9
	4.290	64.0	200	0.16	12.6
	0.764	16.0	300	0.38	17.9
	1.140	21.0	300	0.29	16.9

Table 4. Limiting values for SOF_4 production rates.

Polarity	Discharge Power (W)	Discharge Current (μA)	Gas Pressure (kPa)	Production Rates (n moles/J)	(μ moles/C)
Pos.	0.804	20.0	116	7.02	290
	0.054	1.5	200	7.04	260
	0.335	8.0	200	8.60	373
	0.777	16.0	200	8.45	418
	0.198	4.0	300	5.79	292
	0.430	8.0	300	5.92	343
	0.945	16.0	300	7.08	431
Neg.	0.898	25.0	114	0.85	30.1
	0.230	8.0	200	0.92	23.8
	0.586	16.0	200	0.97	34.6
	0.821	20.0	200	1.05	41.5
	2.215	40.0	200	0.90	49.7
	4.290	64.0	200	0.94	63.6
	0.764	16.0	300	0.44	20.6
	1.140	21.0	300	0.39	21.0

The rate values given in tables 2 and 3 for SOF_2 and SO_2F_2 have been assigned a maximum uncertainty of ±35 percent. The rates for SOF_2 typically have less uncertainty than those for SO_2F_2. Results from positive corona have higher uncertainty than those from negative corona because of the greater fluctuations in the discharge current in the former case. For SOF_4 the uncertainties are higher, but estimated to be always less than ±57 percent. The rates given in table 5 for the minor products are only estimates since a reasonable error assessment was impossible.

Table 5. Estimated production rates for minor species from negative corona in SF_6.

Species	Discharge Current (μA)	Pressure (kPa)	Production Rates	
			(n moles/J)	(μ moles/C)
SO_2	25	114	0.008	0.3
SO_2	40	200	0.002	0.1
OCS	40	200	1.3×10^{-5}	7.2×10^{-3}
CO_2	40	200	0.035	2.0

The results for r_u and r_q are shown in figures 4 and 5 respectively for negative corona at the pressure of 200 kPa. Important observations from the data in tables 2-4 and figures 4 and 5 include:

The production rates for SOF_2, SO_2F_2, and SOF_4 are of comparable magnitude to within roughly a factor of 3. For most cases, particularly at the higher pressures and power levels, the order of production rates is $r_q(SOF_4) > r_q(SOF_2) > r_q(SO_2F_2)$.

Oxyfluoride production does not change dramatically with pressure. One exception is the large relative drop in the SOF_2 and SO_2F_2 rates compared to SOF_4 in going from 200 to 116 kPa for positive polarity.

Oxyfluoride production increases by a factor of five or more in going from negative to positive polarities for discharges of comparable power levels.

The charge rates-of-production for SOF_2 and SO_2F_2 vary less with discharge level than the corresponding energy rates; whereas, the opposite appears to be true for SOF_4.

The trends noted for SOF_2 and SO_2F_2 from the fourth observation imply that the time rates-of-production for these are more nearly directly proportional to the current than the power, i.e., $dc/dt \propto i$. Because of the relatively large uncertainties, it can only be stated that for SOF_4, the rates behave like dc/dt
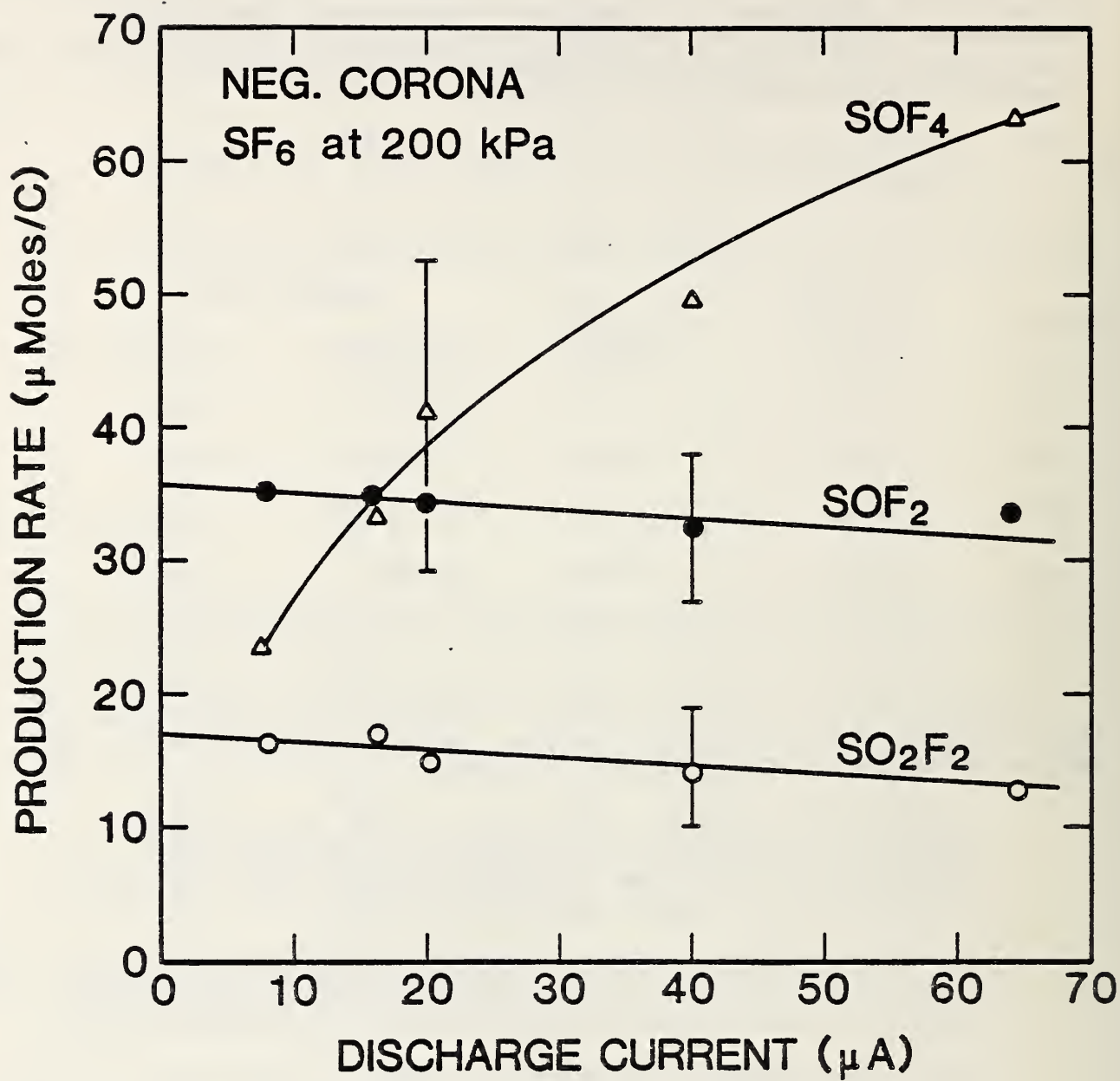
Figure 4. Measured charge rates of production for SOF_4, SOF_2, and SO_2F_2 versus discharge current for negative corona in 200 kPa SF_6.
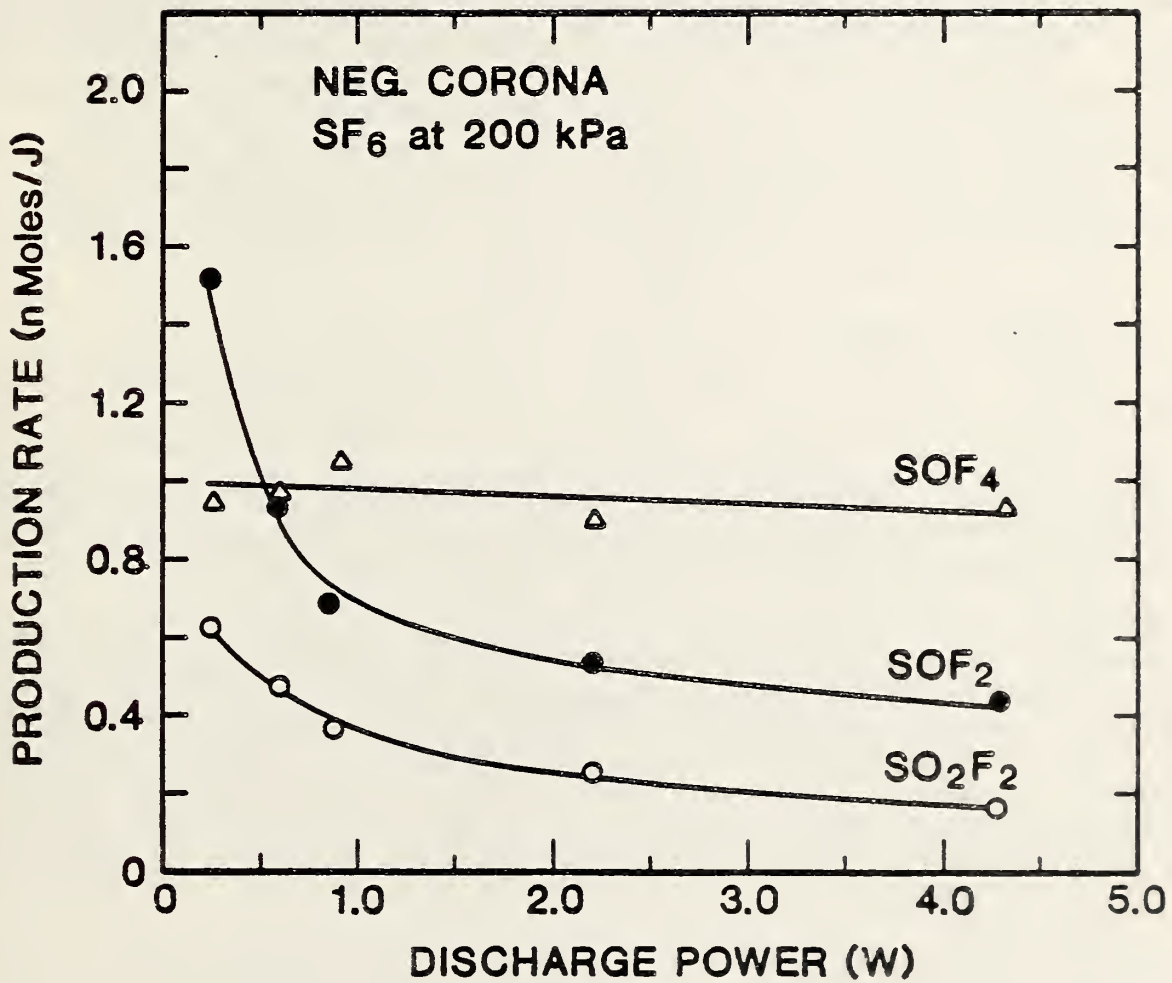
Figure 5. Measured energy rates of production for SOF_4, SOF_2, and SO_2F_2 versus discharge power for negative corona in 200 kPa SF_6.

$\propto i^a$, with $1 < a < 2$. The results in figure 5 would in fact suggest that $dc/dt \propto p$ for this species, where p is the power dissipation in the discharge.

3.2 Comparisons with Previous Observations

The oxyfluoride production rates found here are comparable in magnitude to many of those previously reported in other types of SF_6 electric discharges. However, any comparisons with other results is of questionable significance, since all previous measurements were performed under dissimilar conditions. The configuration used by Chu, et al. [6] was perhaps most nearly like that of the present experiments. These measurements were performed with corona generated by 60-Hz ac voltage applied to aluminum electrodes in SF_6 at a pressure of about 155 kPa. The corona evidently occurred at the peaks of each half-cycle and was mainly characterized by pulses with an average magnitude of 10^3 pC and a repetition rate of 2 kHz. From the information provided, the total $SOF_2 + SO_2F_2$ production rate from this measurement is estimated to lie between 620 and 1400 μ moles/C. The conditions most like this in the present work would correspond to the positive discharge at 1.5 μA which yielded a net rate for $SOF_2 + SO_2F_2 + SOF_4$ production of 592 μ moles/C.

Although the present result is close to that of Chu, et al., it is disturbing that they do not observe SOF_4. It is conceivable that this can be explained by a conversion of SOF_4 to SO_2F_2 via the reaction $SOF_4 + H_2O \rightarrow SO_2F_2 + 2HF$ in the gas sampling process. Other cases [7,8] where there was failure to see SOF_4 from corona or "weak-current" discharges in SF_6, even though SO_2F_2 was reported to be a predominant product, might also be accounted for by hydrolysis of SOF_4. There are documented cases [9-12] where SOF_4 was observed in low-current discharges and even appeared as the dominant product.
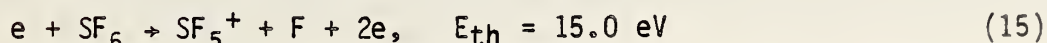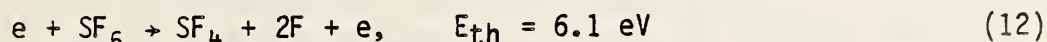
Boudene, et al. [13], Sauers, et al. [14], and Castonguay [15] all report total oxyfluoride energy rates-of-production in SF_6 arcs and sparks with stainless steel electrodes that are comparable in magnitude to some of the rates found here. However, these types of discharges appear to generate predominantly SOF_2. Also, in these cases metal vapors and thermal dissociation may play an important role because of the high levels of power dissipation. The present results are consistent with previous observations and arguments [7,8,16,17] that SO_2F_2 and SOF_4 should become more prevalent as by-products when the discharge power level is reduced.

Recent relative measurements by Ophel, et al. [18], of the total hydrolyzable fluoride production from stainless steel, point-plane corona in flowing SF_6 at 440 kPa show net time rates-of-production that are directly proportional to discharge current rather than power. This behavior would be consistent only with the results found here for SOF_2 and SO_2F_2. Were SOF_4 to become a major component among the hydrolyzable species detected, then the present results indicate that proportionality to current need no longer be expected.

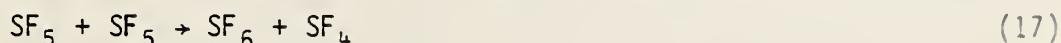## 3.3 Possible Mechanisms for Oxyfluoride Formation

It is useful as a guide in the interpretation of the results to consider the plausible sequences of reactions which can lead to production of SOF_2, SO_2F_2, and SOF_4 in a corona discharge. It should be cautioned, however, that chemical processes in electric discharges are generally expected to be complex,
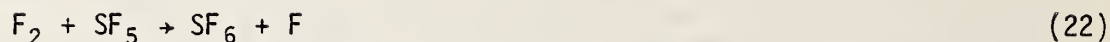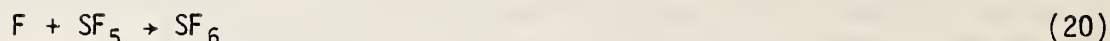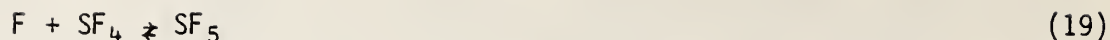
16

involving many intermediate steps. An exhaustive listing of the possible processes is beyond the scope of this work. It is intended here to draw attention to some of the important reactions which appear to be consistent with the present observations and which should be included in any serious attempt to describe the decomposition of SF_6 theoretically. A corona is a relatively weak plasma in which the electron temperature greatly exceeds the gas temperature and nonequilibrium conditions prevail [19]. It is therefore expected that the initial stage of SF_6 decomposition involves dissociation of molecules by electron collisions. At electric field-to-gas density ratios, E/N, close to the critical value where ionization growth is possible, the mean electron energies in an SF_6 discharge are theoretically estimated [20-22] to be between 5 and 10 eV. Thus some of the processes that are likely to contribute include:

$$e + SF_6 \rightarrow SF_5 + F + e, \qquad E_{th} = 4.0 \text{ eV} \qquad (11)$$

$$e + SF_6 \rightarrow SF_4 + 2F + e, \qquad E_{th} = 6.1 \text{ eV} \qquad (12)$$

$$e + SF_6 \rightarrow SF_3 + 3F + e, \qquad E_{th} \sim 9.5 \text{ eV} \qquad (13)$$

$$e + SF_6 \rightarrow SF_2 + 4F + e, \qquad E_{th} \sim 12 \text{ eV} \qquad (14)$$

$$e + SF_6 \rightarrow SF_5^+ + F + 2e, \qquad E_{th} = 15.0 \text{ eV} \qquad (15)$$

$$e + SF_6 \rightarrow SF_5^- + F, \qquad E_{th} \sim 0 \text{ eV}. \qquad (16)$$

Indicated are the threshold energies E_{th} based on determined ionization, attachment, and bond dissociation energies [20-26]. Other processes that can occur include dissociative attachment, leading to F^-, dissociative ionization leading to smaller or multiply charged fragments; and multistep dissociation, e.g., dissociation of the fragments such as $e + SF_4 \rightarrow SF_3 + F + e$. The cross sections or relative probabilities for these processes are expected to be lower than those listed above [21,27]. Of those processes given, the greatest contribution will probably be from dissociation leading to the larger fragments SF_x, x = 3, 4, 5 which is supported by calculations by Masek, et al. [28], of dissociative fragment production rates from electron swarms in SF_6 and SF_6/O_2 mixtures using numerical solutions of the Boltzmann equation. Cross sections for processes (11)-(14) are not known, but are included in the total electronic excitation cross section which is estimated [20-22] to be comparable to or larger than the cross sections for attachment and ionization. The latter processes are not energetically favored for E/N values near the ionization limit since attachment probabilities are peaked at very low energies where the electron energy distribution function rapidly decreases, and the thresholds for ionization occur in the high energy tail of the distribution. The thresholds for the favored dissociation processes occur near the peak of the energy distribution.

It is known [9] that if oxygen containing species are not present in the gas or on surfaces to react with the SF_6 dissociation products, then they will rapidly recombine through relatively fast processes such as

$$SF_5 + SF_5 \rightarrow SF_6 + SF_4 \qquad (17)$$

$$SF_5^+ \rightarrow SF_4^+ + F \qquad (18)$$

$$F + SF_4 \rightleftharpoons SF_5 \tag{19}$$

$$F + SF_5 \rightarrow SF_6 \tag{20}$$

$$F_2 + SF_4 \rightarrow SF_5 + F \tag{21}$$

$$F_2 + SF_5 \rightarrow SF_6 + F \tag{22}$$

The list, of course, represents only a portion of the possible reactions. The reaction sequence (19)-(22) has been proposed by Gonzalez and Schumacher [29] to explain the observed rapid thermal conversion of $SF_4 + F_2$ into SF_6. It has been argued [30] that reaction (17) is favored because of its low activation energy. The enthalpy change ΔH°_{298} for this reaction is -49.4 kJ/mole. From available thermochemical data [31], one obtains ΔH°_{298} = -434.1 kJ/mole for either sequence (19)-(22) or (17) and (19)-(21). There is evidence [32] from mass spectral data that SF_5^+ can be formed in metastable states that decay according to (18). The ions SF_4^+ and SF_5^+ are expected to be highly reactive.

Other reactions among the SF_6 products can yield long-lived sulfur fluorides like S_2F_2 and S_2F_{10}. Both of these have been reported as minor products of SF_6 decomposition in some arc or spark discharge studies [16]. It is known [33] that S_2F_2 (and its isomers) are more likely formed by the reaction

$$S + SF_2 \rightarrow S_2F_2, \tag{23}$$

rather than

$$SF + SF \rightarrow S_2F_2. \tag{24}$$
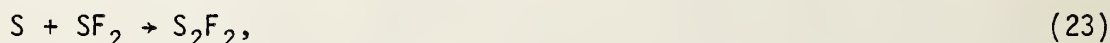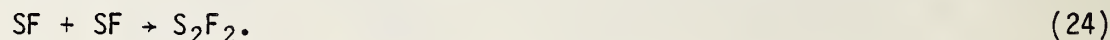
Formation of S_2F_2 is thus not expected in a cool discharge which yields predominantly the larger SF_x fragments. It is reported [29] that although S_2F_{10} can be formed by the reaction

$$SF_5 + SF_5 \rightarrow S_2F_{10}, \tag{25}$$
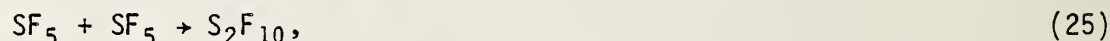
its rate is much lower than those of the competitive reactions (17) or (19)-(22). The product S_2F_{10} is important because of its high toxicity [13,17]. Due to its thermal instability, it could not be observed by the present chromatographic method. The species SF_4 is reported to be the most stable and most abundant primary product from both thermal dissociation of SF_6 at moderate temperatures [34-36] and from relatively cool electric discharges [37,38]. The SF_5 radical has not been observed even at relatively low temperatures, and this suggests that the reactions which convert it to SF_4 and SF_6 are quite fast.

The presence of oxygen, or oxygen containing species in the discharge region will interfere with the recombination process and give rise to the formation of oxyfluorides, free fluorine, and HF. Possible, energetically favorable, bimolecular reactions that could directly lead to oxyfluoride formation in the discharge are [39]:

$$SF_5 + OH \rightarrow SOF_4 + HF, \qquad \Delta H^\circ_{298} = -464 \text{ kJ/mole} \tag{26}$$

$$SF_5 + O \rightarrow SOF_4 + F, \qquad \Delta H^\circ_{298} = -327 \text{ kJ/mole} \tag{27}$$

$$SF_4 + O \rightarrow SOF_4, \qquad \Delta H°_{298} = -549 \text{ kJ/mole} \tag{28}$$

$$SF_4 + O \rightarrow SOF_2 + 2F, \qquad \Delta H°_{298} = -124 \text{ kJ/mole} \tag{29}$$

$$SF_3 + O \rightarrow SOF_2 + 2F, \qquad \Delta H°_{298} = -213 \text{ kJ/mole} \tag{30}$$

$$SF_2 + O \rightarrow SOF_2, \qquad \Delta H°_{298} = -496 \text{ kJ/mole} \tag{31}$$

$$SF_4 + OH \rightarrow SOF_2 + HF + F, \quad \Delta H°_{298} = -130 \text{ kJ/mole} \tag{32}$$

$$SF_3 + OH \rightarrow SOF_2 + HF, \qquad \Delta H°_{298} = -351 \text{ kJ/mole} \tag{33}$$

$$SF_3 + O_2 \rightarrow SO_2F_2 + F, \qquad \Delta H°_{298} = -260 \text{ kJ/mole} \tag{34}$$

$$SF_2 + O_2 \rightarrow SO_2F_2, \qquad \Delta H°_{298} = -461 \text{ kJ/mole} \tag{35}$$

Reactions (29), (30), and (34) have previously been invoked [40,41] to account for rapid SOF_2 and SO_2F_2 formation from pyrolysis of SF_6 in the presence of O_2. Reactions (27)-(30) have been mentioned by d'Agostino and Flamm [9] as mechanisms for oxyfluoride production from SF_6/O_2 mixtures in low-pressure, rf discharges. Leipunskii, et al. [30] have mentioned reaction (32) and suggested that it proceeds through the intermediate SOF_3.

From low-pressure SF_6/O_2 mixtures with relatively high O_2 content there is evidence [29,42,43] that ion and neutral species such as SOF_3^+, $SO_2F_3^+$, $SO_2F_5^+$, $S_3OF_7^+$, SF_5O_2, SF_5O, $SF_5O_2SF_5$, and $SF_5O_3SF_5$ are also formed. Some of these may act as intermediates in the formation of the observed oxyfluorides. Because of the relatively high pressures and low oxygen content in the present experiments, it can be argued [29] that formation of large sulfur oxyfluorides such as $SF_5O_3SF_5$ is unlikely.

If the concentrations of the by-products become sufficiently high, then secondary reactions can play a role in the discharge. Included here are reactions such as

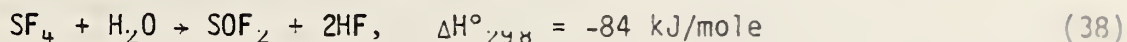$$SOF_2 + O \rightarrow SO_2F_2, \tag{36}$$
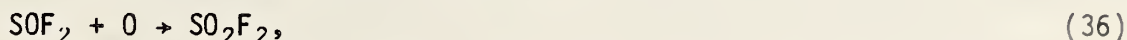
whereby the stable oxyfluorides undergo conversion from attack by free radicals or ions generated in the discharge. Because the observed oxyfluorides always remained at trace levels, reactions of this type are expected to be unimportant here provided that they are confined to the small volume of the discharge.
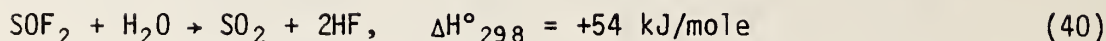
Secondary reactions involving SF_6^- in the ion drift region could be more important. A possibly significant reaction is the F^- exchange

$$SF_6^- + SOF_4 \rightarrow SOF_5^- + SF_5 \tag{37}$$
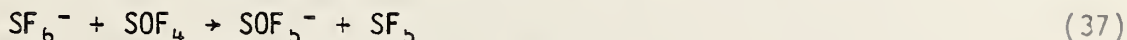
which affects SOF_4 production.

Within the bulk of the gas or on the walls, slower reactions may occur which would modify the gas composition. Processes in this catagory are:

$$SF_4 + H_2O \rightarrow SOF_2 + 2HF, \quad \Delta H°_{298} = -84 \text{ kJ/mole} \tag{38}$$

$$SOF_4 + H_2O \rightarrow SO_2F_2 + 2HF, \quad \Delta H^\circ_{298} = -2 \text{ kJ/mole} \tag{39}$$

$$SOF_2 + H_2O \rightarrow SO_2 + 2HF, \quad \Delta H^\circ_{298} = +54 \text{ kJ/mole} \tag{40}$$
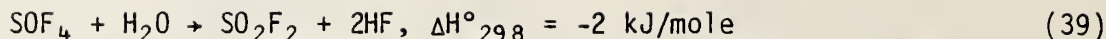
All of the reactions (38)-(40) are possible at room temperature. However, consistent with the present results, only reaction (38) is rapid enough to significantly influence the observed oxyfluoride production. Its rate has been estimated by Sauers, et al. [37] to lie between 1.0 and 2.6 x 10^{-19} cm^3/s at a temperature of 350 K. Assuming that this is a gas phase reaction, and using typical water vapor concentrations found in the present experiments, it is estimated that SF_4 has a half-life in the cell of between 0.15 and 0.40 h. Since this is small compared to typical gas sampling intervals, it can be assumed that SF_4 is completely converted to SOF_2. Reaction (38) has frequently been invoked to account for SOF_2 production in previous investigations of SF_6 decomposition; however, it has never been verified that it is actually a gas-phase reaction. If it does occur in the gas phase, then most likely, as suggested by Herron [39], it proceeds through the intermediate SF_3OH in two steps.

Reaction (39) has previously been proposed [13-17] to explain SO_2F_2 production in electric discharges. The present results indicate that its rate in the gas phase is too slow to account for most of the SO_2F_2 formed. It could nevertheless, as noted above, explain the absence of gaseous SOF_4 in some earlier experiments. The extremely low rate of SO_2 production [5] suggests furthermore that reaction (40) is also not important for the conditions considered here.

It is evident from consideration of reactions (34) and (35), that production of SO_2F_2 directly from primary SF_6 dissociation products requires O_2. The important role of O_2 in enhancing SO_2F_2 production has been verified in earlier work [9,13,30,44], and is consistent with the present observations. For decomposition at lower pressures [9], addition of O_2 appears to increase SO_2F_2 production at the expense of SOF_4. Boudene, et al. [13] noted that both SO_2F_2 and SOF_4 production rates in high-pressure arcs are more sensitive to gas-phase O_2 content than SOF_2 production.

Failure to observe significant quantities of SO_2F_2 and SOF_4 in high-temperature arcs could be accounted for in part by the higher degree of gas dissociation in these cases compared to low-power discharges. Certainly it could be expected that availability of undissociated oxygen and the larger SF_x fragments would be reduced at higher temperatures so as to inhibit reactions (26)-(35). This hypothesis is supported by equilibrium calculations at high temperatures [34,40]. Since SOF_2 could be produced primarily by reaction (38), its formation need not depend on O_2 content. The fact that SO_2F_2 is generally observed here and by others [9,10,30,40] to have the lowest rate of formation in relatively low-temperature or low-power SF_6 decomposition processes can be understood by its dependence on the availability of the lower valence SF_3 and SF_2 fragments. In cool discharges these are likely to be produced with lower probabilities than the larger fragments SF_4 and SF_5 which would preferentially convert to SOF_4 and SOF_2.

3.4 Influence of O_2 and H_2O on Oxyfluoride Production

The sources from which oxygen is derived for production of SOF_2, SO_2F_2, and SOF_4 have not been positively identified in the present experiments, although

measurements are now underway that could significantly narrow the range of possibilities. The following three sources deserve consideration: 1) gaseous O_2 contamination including that initially present plus that introduced during discharge operation; 2) oxygen contained on surfaces including that which is chemically bound in insulating materials such as SiO_2; 3) H_2O present either in the gas or on surfaces. Interpretation of the present results suggests that the primary oxygen sources are not necessarily the same for all species. Source (2) will be considered unimportant in the discussion that follows because of the highly confined nature of the discharge which was located far from insulating surfaces.

At least at low levels (less than 1 percent), the measurements show that oxyfluoride production is not extremely sensitive to variations in the gas phase O_2 and H_2O concentrations. In fact, when O_2 content was increased above 10%, total oxyfluoride yield decreased. This implies that the production rates are controlled mainly by the dissociation rates of SF_6, i.e., by the availability of SF_x fragments. The decrease in oxyfluoride yield with increasing O_2 content may be due to the influence of O_2 on the SF_6 dissociation rate, e.g., by modification of the electron energy distribution as suggested by Masek [28]. The observed [5] consumption of gaseous H_2O can be accounted for by its role in SOF_2 formation through reaction (37) and by providing O and OH radials for reactions (26)-(33) in the discharge.

It is proposed on the basis of the foregoing discussion that the primary oxygen sources for SOF_2 and SO_2F_2 could be derived respectively from H_2O and O_2, whereas SOF_4 could derive oxygen from both of these. This assignment is strengthened by the interpretation of the dependences of the rates on discharge current and time as discussed below.

3.5 Dependence of Oxyfluoride Production on Discharge Current and Time

The condition $dc/dt \propto i$, observed here for SOF_2 and SO_2F_2, is expected if: 1) the formation process involves only one electron impact generated dissociation fragment; and 2) changes in i do not significantly modify the electron energy distribution in the discharge. The first condition is satisfied by the predominant mechanisms suggested above to account for SOF_2 and SO_2F_2 production. The second condition is open to question, but is evidently a reasonable assumption [19] for glow or corona-type discharges in which the electric field is controlled by ion space charge. Increases in applied voltage required to increase the current will presumably expand the volume of space charge without significantly altering the mean E/N. Independent of i and corresponding space charge development, dissociation is expected to occur predominantly in regions of comparable E/N.

Certainly if $dc/dt \propto i$ for SOF_2 and SO_2F_2, then it is expected, on the basis of the proposed mechanisms, that $dc/dt \propto i^2$ for SOF_4, since its formation involves two fragments from electron impact dissociation. The production of SOF_4 increases with i as seen in figure 4, but probably somewhat more slowly than i^2. The deviation from i^2 dependence, if significant, could be accounted for by secondary reactions such as reactions (37) and (39) which could remove SOF_4.

As production of SOF_4 becomes predominant, it might be expected to affect the product rates of the other oxyfluorides since it competes in the consumption

of SF_4 and SF_5. Rates for both SOF_2 and SO_2F_2 show a slow fall off with increasing i which may indicate competition with SOF_4 production. The extent to which SOF_4 production is competitive depends, however, on the extent to which it preferrentially consumes free radicals used in SOF_2 or SO_2F_2 formation as opposed to those that would otherwise recombine.

If the initial portions of the production curves are ignored [5] and it is assumed that the curves do indeed approach linearity, then reactions involving initial gas dissociation products would appear to dominate in oxyfluoride production. Deviations from linearity can occur if secondary reactions contribute by which one oxyfluoride is transformed into another, e.g., reactions (36) and (39). Because of the low oxyfluoride content, reactions such as (36) which occur in the discharge are considered unlikely, and measurements made at times when the discharge was off indicate that reactions like (39) and (40) that could occur in the bulk of the gas are too slow to observe.

3.6 Polarity Effect

The large effect of reversing polarity on the production rates of the oxyfluorides can be understood from consideration of corresponding pronounced changes in the discharge characteristics [45]. In evaluating this effect the following observations are noted: 1) the effect is greater for SO_2F_2 and SOF_4 than for SOF_2; 2) the power dissipation at a given current was always higher for positive polarity; 3) the discharge was more pulsating under positive polarity; and 4) the point electrode surface suffered considerably more damage under positive polarity. In positive discharges the point electrode surface is evidently subjected to bombardment by more highly energetic ions or electrons from electron avalanches originating in the gas than is the case in negative discharges where a more uniform ion space charge is effective in shielding the electrode surface and moderating the energies of impacting ions. Higher mean electron energies and higher electrode surface temperatures would be consistent with a higher dissociation rate in the positive case. In addition to dissociation by electron impact, pyrolysis of SF_6 at the positive point surface could conceivably contribute to decomposition. The enhancement in oxyfluoride production in going from positive to negative polarity is consistent with the postulated increase in the gas dissociation rate.

Greater heating of the electrode in the positive case could also be accompanied by a higher rate of oxygen release into the discharge volume. This would influence oxyfluoride production and might account for a more pronounced effect for the species SO_2F_2 and SOF_4 that, according to the above model, are most affected by the presence of oxygen.

3.7 Magnitude of Production Rates

Information is not available at the present time on the rates for all of the various chemical processes invoked here to account for oxyfluoride production. Thus, accurate predictions of the production rates are not yet feasible. Nevertheless, sufficient information does exist to at least allow upper limits to be placed on the magnitude of the total SF_6 decomposition rates for discharges in which dissoication is controlled mainly by electron collision processes. Based on the evidence provided here that the rate determining factor is the initial SF_6 dissociation rate, i.e., the rate for processes such as

$$e + SF_6 \rightarrow SF_x + (6-x)\ F + e, \qquad (41)$$

then an upper limit on the total oxyfluoride yield can be estimated using the following two assumptions: 1) all SF_x fragments convert to oxyfluorides; and 2) electronic excitation leads predominantly to dissociation so that the total electronic excitation rate k_{ex} coincides with the total dissociation rate. The rate k_{ex} could also be adjusted to include fragmentation of SF_6 leading to various ion products.

In addition, a one dimensional approximation is made that electrons released into the active ionization volume at a constant rate dn_e/dt, e.g., by field emission from the point cathode, traverse the gap distance d along the point-to-plane axis. These assumptions enable one to compute the total charge rate-of-production $r_{q,t}$ defined by

$$r_{q,t} = \sum_{i=1}^{3} r_{q,i} \qquad (42)$$

where the $r_{q,i}$ are the rates for the individual oxyfluoride components. Allowing for the variations of electron production in the gap by ionization and attachment, one obtains the expression

$$r_{q,t} = i^{-1}(N/N_0)(dn_e/dt) \int_0^d \frac{k_{ex}(\ell)}{\bar{v}(\ell)}\ \exp\left[\int_0^\ell (\alpha(\ell')-\eta(\ell'))d\ell'\right]\ d\ell, \qquad (43)$$

where α and η are respectively the usual ionization and attachment coefficients [16-18], $\bar{v}$ is the electron drift velocity, and N_0 is the Avogadro constant required to express the rate in units of moles-per-coulomb. In general, the quantities k_{ex}, v, α, and η will depend on E/N and hence on position ℓ' in the gap.

Precise variations of E/N within the gap are not easily predicted when the discharge is present due to the expected strong influence of ion space charge on the field. However, the active region near the point in which signficant ionization and excitation occur must satisfy the condition

$$\alpha(\ell') > \eta(\ell'). \qquad (44)$$

When this condition no longer holds, electrons are quickly thermalized and removed from the gas by attachment to SF_6 molecules. Lacking knowledge of the exact dependence of E/N on ℓ', the active discharge volume will be modeled here as a region of extent ℓ in which eq (44) holds, and E/N assumes a constant value close to the critical value $(E/N)_c$ where $\alpha = \eta$. This choice takes into consideration the expected moderating effect of the ion space charge which tends to reduce the field near the point.

Expressing N in terms of pressure p and temperature T using $N = p/kT$ (k is the Boltzmann constant), the approximation for $r_{q,t}$ becomes

$$r_{q,t} \simeq \frac{\bar{k}_{ex}p\ell}{e\bar{v}kT}\ \frac{1}{N_0}\ , \qquad (45)$$

where e is the electron charge, and k_{ex} and $\bar{v}$ assume the values for the electronic excitation rate coefficient and drift velocity respectively at $E/N \sim (E/N)_c = 370 \times 10^{-21}$ Vm^2 corresponding to the known [46] critical value for SF_6. · In deriving eq (45) it is assumed that the measured discharge current i corresponds to electron motion only. It should be noted that l is, in general, pressure dependent so that $r_{q,t}$ may not be proportional to pressure as implied by eq (45).

There appears to be some disagreement in the literature [20,21,47] about the correct total electronic excitation cross sections needed to determine the rate coefficient k_{ex} for SF_6. It will be assumed here that

$$2 \times 10^{-15} \text{ m}^3/\text{s} \geq k_{ex} \geq 1 \times 10^{-15} \text{ m}^3/\text{s},$$

where the lower value corresponds to that calculated by Masek, et al. [28] at $E/N = 100 \times 10^{-21}$ Vm^2 and the upper value allows for the expected increase in k_{ex} for $E/N = (E/N)_c$. The values of k_{ex} considered here are comparable in magnitude to those reported in the literature for other molecules [48]. The observed [46] value for $\bar{v}$ in SF_6 at $(E/N)_c$ is about 2×10^5 m/s. The extent of the active region is expected [49] to lie between about 1 and 2 percent of the total gap spacing, i.e., 0.24 mm > ℓ > 0.12 mm. Using eq (45), the predicted upper limit on the rate for a pressure of 200 kPa and temperature of 300 K lies in the range, 1800 μmoles/C > $r_{q,t}$ > 450 μmoles/C. This can be compared with the values obtained from tables 2-4 for a pressure of 200 kPa. For positive discharges at 8.0 μA and 16.0 μA respectively, it is found, for example, that $r_{q,t}$ = 634 μmoles/C and $r_{q,t}$ = 717 μmoles/C, and for a negative discharge at 40 μA, $r_{q,t}$ = 96 μmoles/C.

The results for positive discharges generally lie within the range of predicted upper limit values, whereas results for negative discharges lie well below the range. It should be noted that the model used is perhaps more appropriate for negative discharges where electrons originate from the point electrode surface and the space charge is expected to be uniformly distributed about the point. For positive discharges, the space charge is probably much less uniform, and as previously suggested, there may be contributions to dissociation from processes other than electron impact.

Undoubtedly, the mean value of E/N in the active volume is greater than $(E/N)_c$ for the positive case. However, independent of polarity, the total rates $r_{q,t}$ do not, and should not, lie significantly above the range of upper limits estimated here.

During the next quarter emphasis will be given to activity 2). Further measurements will be made on oxyfluoride production from SF_6/O_2 mixtures in negative corona. These investigations will also be extended to SF_6/N_2 mixtures for which nitrogen oxide as well as oxyfluoride production rates will be measured as a function of N_2 content.

For further information contact Dr. R. J. Van Brunt at (301) 921-3121.

4. NANOSECOND BREAKDOWN IN POWER SYSTEM DIELECTRICS

The objectives of this effort are to develop measurement capabilities and to provide data in support of the DOE program concerned with the effects of fast rising electrical signals on electric power systems.

The response of the dielectric components of electrical equipment to waveforms such as those generated by lightning or switching surges is reasonably well understood. However, there exists only a limited set of information regarding breakdown phenomena when dielectrics are subjected to fast rising pulses such as those generated by nuclear electromagnetic pulses or by disconnect operations in gas insulated equipment. Conventional equipment used in breakdown studies is, at best, marginally adequate for use in nanosecond breakdown studies. Test facilities must provide suitable pulse shapes, test cell geometries, and electrical diagnostics with time resolution in the nanosecond range.

The test facility shown schematically in figure 6 illustrates some of the features which must be an integral part of a system which is to be used to study sub-microsecond breakdown in dielectric materials. The pulse forming network and triggered switch provide the desired voltage waveform, the test cell contains the dielecric specimen, and, in the transmission line shown in figure 6, the termination prevents a reflected wave from being imposed across the test cell. While not all systems will have this appearance, the salient features must be the same. Of critical importance are the voltage and current sensors indicated, since accurate measurements are required to determine both the voltage and temporal characteristics of breakdown in the dielectrics. If, for example, the effects of trace impurities on formative time lags in SF_6 are of interest, then both the voltage at which breakdown occurs and the time to breakdown after application of the voltage pulse must be determined. Since these time lags may be as short as 1-2 nanoseconds, severe requirements are placed on the voltage sensors. In addition to experimental studies in the laboratory, the use of analytical techniques to characterize these sensors appears necessary.

The characterization of sensors and many other electrical measurement devices such as waveform recorders can, under rather general conditions, be reduced to deconvolving an integral equation. We present a method of deconvolution and discuss its applicability to the problem of sensor characterization.

In our laboratory an input signal, $x(t)$, to and an output signal, $y(t)$, from a device are recorded (see figure 7). When such a system is linear, causal, and time-shift invariant, linear systems theory allows one to infer that

$$y(t) = \int_0^t x(s) \ g \ (t-s) \ ds \tag{46}$$

where g is the impulse response of the system [50].

Equation (46) can be the basis for determining g or its integral, the step response $S(t)$. Alternatively, one may determine the input signal, x, if y and either g or S are known. Mathematically and computationally these two problems may be solved by identical means.

The principal difficulty in the solution of eq (46) is that one has an integral of the first kind which is singular or nearly so. In our case, the data x and y are finite collections of discrete, digitized measurements and are subject to error. When discretized, eq (41) gives rise to a linear equation
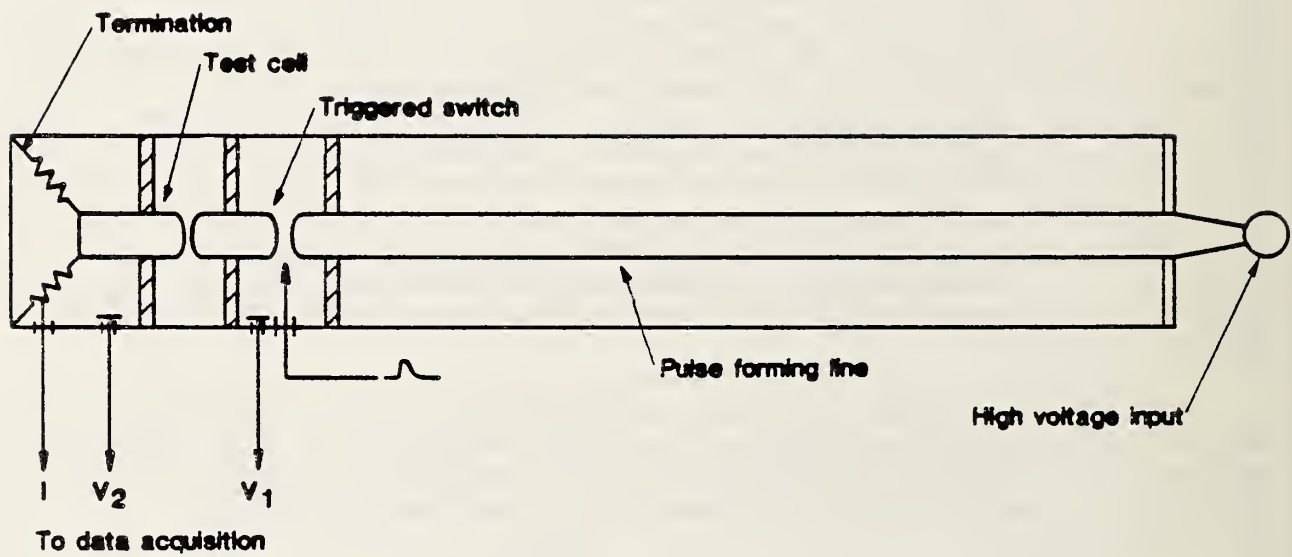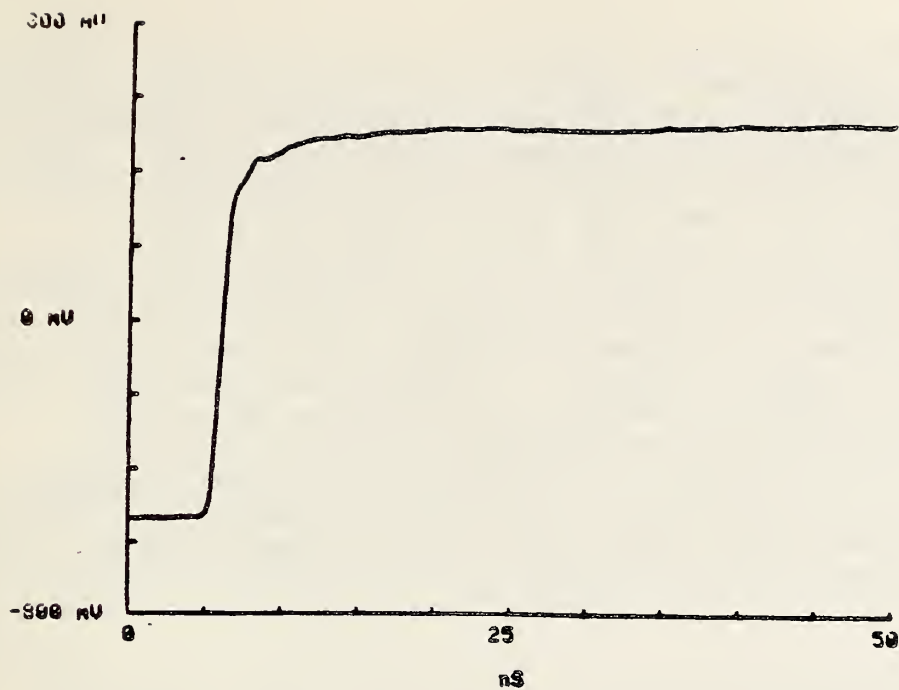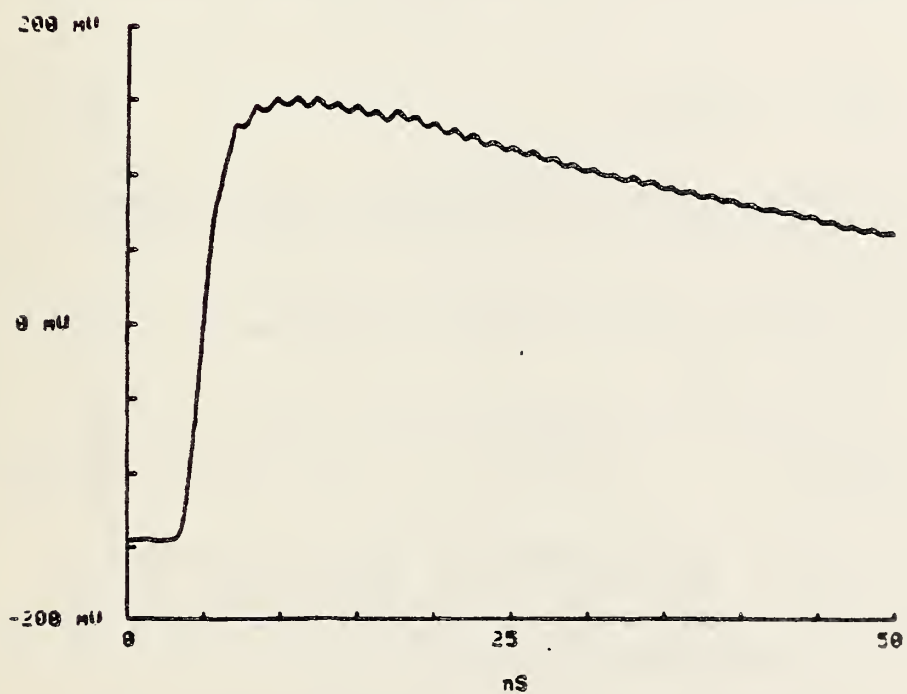
25

Figure 6. Schematic representation of transmission line pulse generator to study fast risetime breakdown processes in dielectrics.

Figure 7. Examples of input-output pairs used in deconvolution studies of
           capacitive voltage sensors. Data were acquired using a fast waveform
           recorder. (a) output from mercury wetted relay pulser. (b) output
           from sensor under test.

27

$$X \, g = y \tag{47}$$

which may be non-singular but is ill-conditioned. Thus eq (47) has a unique solution, g, but small variations in y produce large variations in g. Such variations are a characteristic of noisy systems. Because eq (47) is ill-conditioned we consider that the system to be solved has the form

$$X \, g = y_\tau + n \, , \tag{48}$$

where n is noise superimposed on the true output, y_τ. If we knew y_τ we might find g_τ (the correct impulse response). Of course, one can't know y_τ. In effect this means there is a large class of solutions to eq (48). From this class we seek functions, g, which satisfy auxillary, a priori conditions. These are typically that g or its derivatives are not too large. Intuitively, these conditions require that g not be wildly oscillatory. One may use as a measure of size some combination of the root mean square (RMS) magnitudes of g and its derivatives, for example,

$$\left\| Rg \right\| = \left\| \frac{d^2}{dt^2} \, g \right\|_2 . \tag{49}$$

R is called a regularizing operator and $\left\| \cdot \right\|_2$ is the RMS norm [51]. We then seek solutions to the regularized version of eq (42) by finding γ_r which minimizes

$$\left\| y - Xg \right\|_2^2 + \gamma_r \left\| Rg \right\|,^2 \tag{50}$$

γ_r is a positive number called a regularization parameter. Thus we abandon exact data consistency for a combination of faithfulness to the data and reasonableness of the solution.

An equivalent linear problem is given by the Euler equation for eq (50)

$$(X^T X + \gamma R^2) \, g = X^T y. \tag{51}$$

We solve eq (51) using a variety of R's (identity and first difference operators as well as the R given above).

The results of these calculations for model data derived by perturbing analytic functions are very good. For experimentally derived data, initial results suggest that the numerical method can construct g_r close to the limits of detectability imposed by the measurement of x and y.

The utility of this technique is limited by the absence of error bounds or other measures of the sensitivity of g_r to noise in x and y. The digitizer we use has a frequency response which is flat to about 400 megahertz, and which has a system rise time of 0.8 ns.

We have computed the discrete Fourier transform (DFT) for the x and y. Above 2 Ghz the noise-to-signal ratio is high, judging by the variation observed in repeat shots. Meaningful data above 1 Ghz would not be expected, and it is unknown what the transient response of the waveform actually is. Other staff

28

members of the Electrosystems Division are actively pursuing methods which can be used to characterize waveform recorders. The solution of the regularized problem, eq (50), effectively filters high frequency components of the solution vector g_r. The amount of filtering is dependent on the parameter n the selection of which is not directly related to the noise.

One area of investigation in the next year is the inclusion of error estimates in the computation of g. One method of finding confidence intervals is based on the work of O'Leary and Rust [52]. Their methods are not entirely appropriate to the general problem of finding g. A second method is to relate n to the noise, n.

A second area of study is the fast computation of g_r. The storage requirements of the current algorithm are proportional to N^2 and the computation time to N^3 when x and y each has N measurements. We will apply the conjugate gradient method of Hestenes [53]. The storage requirements of our implementation are proportional to N, and by exploiting the structure of eq (46) we reduce the computation time to no more than N^2 log N Both are substantial savings.

In addition to the future analytical work, experimental work will continue on the development of a general system and the adaptation of existing equipment to look at fast breakdown in dielectric liquids.

For further information, contact Dr. R. H. McKnight at (301) 921-3121.

5. REFERENCES

[1] Sir Horace Lamb, Hydrodynamics (Sixth Edition), Dover (1945).

[2] G. K. Batchelor, An Introduction to Fluid Dynamics, Cambridge University Press (1967) (Chapter II).

[3] NBS Report NBSIR 83-2761, Development of Power Systems Measurements-- Quarterly Report, January 1 - March 31, 1983.

[4] R. J. Van Brunt and W. E. Anderson, "Bibliography of Data on Electrical Breakdown in Gases," NBS Tech Note 1185 (1984).

[5] R. J. Van Brunt, T. C. Lazo, and W. E. Anderson, "Production Rates for Discharge Generated SOF_2, SO_2F_2, and SO_2 in SF_6 and SF_6/H_2O Mixtures," Gaseous Dielectrics IV (L. G. Christophorou, ed.) Pergamon Press, New York (1984) pp. 276-285.

[6] F. Y. Chu, H. A. Stuckless, and J. M. Braun, "Generation and Effects of Low Level Contamination in SF_6-Insulated Equipment," Gaseous Dielectrics IV (L. G. Christophorou, ed.) Pergamon Press, New York (1984) pp. 462-472.

[7] H. Grasselt, W. Ecknig, and H. J. Polster, "Application of Gas Chromatography to the Development of SF_6-Insulated Switch Gear and Apparatus," Elektrie, Vol. 32, pp. 398-371 (1978).

[8] F. B. Waddington and J. Heighes, "Sulphur Hexafluoride Insulation for Current Transformers," AEI Eng., Vol. 7, pp. 196-199 (1967).

[9] R. d'Agostino and D. L. Flamm, "Plasma Etching of Si and SiO_2 in SF_6-O_2 Mixtures," J. Appl. Phys., Vol. 52, pp. 162-167 (1981).

[10] G. Bruno, P. Capezzuto, and F. Cramarossa, "Inorganic Volatile Fluorides Obtained from Electrical Decomposition of Sulfur Hexafluoride in a Quartz Tube," J. Fluor. Chem., Vol. 14, pp. 115-129 (1979).

[11] H. J. Emeleus and B. Tittle, "Synthesis of Pentafluorosulphur Chloride and Sulphur Oxide Tetrafluoride in the Microwave Discharge," J. Chem. Soc., pp. 1644-1647 (1963).

[12] H. Gutbier, "Mass Spectrometric Investigation of the Decomposition of Sulfur Hexafluoride in a Glow Discharge," Phys. Verh., Vol. 17, pp. 163 (1966).

[13] C. Boudene, J. Cluet, G. Keib, and G. Wind, "Identification and Study of Some Properties of Compounds Resulting from the Decomposition of SF_6 under the Effect of Electrical Arcing in Circuit Breakers," Rev. Gen. Electr., No. Special, pp. 45-78 (1974).

[14] I. Sauers, L. G. Christophorou, and S. M. Spyrou, "Negative Ion Formation in SF_6 Spark By-Products," Gaseous Dielectrics IV (L. G. Christophorou, ed.) Pergamon Press, New York (1984) pp. 292-305.

[15] J. Castonguay, "Kinetics of the Arc-Decomposition of SF_6-Gas Mixtures,"
Conf. Record, IEEE Int'l Symp. on Elect. Insul., Boston (1980).

[16] W. Becher and J. Massonne, "Contribution to the Decomposition of Sulfur
Hexafluoride in Electric Arcs and Sparks,"Elektrotech. Z. Ausg., Vol. A91,
pp. 605-610 (1970).

[17] A. Baker, R. Dethlefsen, J. Dodds, N. Oswalt, and P. Vouros, "Study of Arc
By-Products in Gas-Insulated Equipment," Elec. Power Res. Inst. Rept.,
EPRI-EL-1648 (1980).

[18] T. R. Ophel, D. C. Weisser, A. Cooper, L. K. Fifield, and G. D. Putt,
"Aspects of Breakdown Product Contamination of Sulphur Hexafluoride in
Electrostatic Accelerators," Nuc. Instr. and Methods, Vol. 217,
pp. 383-396, (1983).

[19] M. Goldman and A. Goldman, in Gaseous Electronics, Vol. 1, (N. M. Hirsh
and H. J. Oskam, ed.) Academic Press, New York (1980) pp. 219-290.
A. Goldman and J. Amouroux, in Electrical Breakdown and Discharges in
Gases, (E. E. Kunhardt and L. H. Luessen, ed.) Plenum Press, New York
(1981) pp. 293-346.

[20] H. Itoh, M. Shimozuma, and H. Tagashira, "Boltzmann Equation Analysis of
the Electron Swarm Development in SF_6 and Nitrogen Mixtures," J. Phys. D:
Appl. Phys., Vol. 13, pp. 1201-1209 (1980); T. Yoshizawa, Y. Sakai,
H. Tagashira, and S. Sakamoto, "Boltzmann Equation Analysis of the
Electron Swarm Development in SF_6," J. Phys. D: Appl. Phys., Vol. 12,
pp. 1839-1852 (1979).

[21] L. E. Kline, D. K. Davies, C. L. Chen, and P. J. Chantry, "Dielectric
Properties for SF_6 and SF_6 Mixutres Predicted from Basic Data," J. Appl.
Phys., Vol. 50, pp. 6789-6796 (1979).

[22] M. S. Dincer and G. R. Govinda Raju, "Monte Carlo Simulation of the Motion
of Electrons in SF_6 in Uniform Electric Fields, "J. Appl. Phys., Vol. 54,
pp. 6311-6316 (1983).

[23] A. P. Modica, "Shock Tube Study of Sulfur Hexafluoride and Sulfur Chloride
Pentafluoride Equilibrium Decomposition," J. Phys. Chem., Vol. 77,
pp. 2713-2719 (1973).

[24] P. J. Hay, "Generalized Valence Bond Studies of the Electronic Structure
of SF_2, SF_4, and SF_6," J. Am. Chem. Soc., Vol. 99, pp. 1003-1012 (1977).

[25] D. L. Hildenbrand, "Mass Spectrometric Studies of Some Gaseous Sulfur
Fluorides," J. Phys. Chem, Vol. 77, pp. 897-902 (1973).

[26] L. M. Babcock and G. E. Streit, "Ion-Molecule Reactions of SF_6:
Determination of I. P.(SF_5), A. P.(SF_5^+/SF_6), and $D(SF_5-F)$," J. Chem.
Phys., Vol. 74, pp. 5700-5706 (1981).

[27] T. Stanski and B. Adamczyk, "Measurements of Dissociative Ionization Cross
Section of SF_6 by Using Double Collector Cycloidal Mass Spectrometer,"
Int. J. Mass. Spec. Ion Phys., Vol. 46, pp. 31-34 (1983).

[28] K. Masek, L. Laska, V. Perina, and J. Krasa, "Some Peculiarities of the SF_6 and the $SF_6 + O_2$ Discharge Plasma," Acta. Phys. Slov., Vol. 33, pp. 145-150 (1983).

[29] A. C. Gonzalez and H. J. Schumacher, "The Kinetics and the Mechanism of the Thermal Reaction between Sulfurtetrafluoride and Fluorine," Z. Naturforsch., B: Anorg. Chem., Org. Chem., Vol. 36B, pp. 1381-1385 (1981).

[30] I. O. Leipunskii, A. K. Lyubimova, A. A. Nadeikin, A. I. Nikitin, and V. L. Tal'roze, "Investigation of the Process of Formation of Oxygen-Containing Products as a Result of Multiphoton Dissociation of SF_6 by Radiation from a High-Power Pulsed CO_2 Laser," Sov. J. Quantum Electronics, Vol. 12, pp. 413-417 (1982).

[31] D. D. Wagman, W. H. Evans, V. B. Parker, R. H. Schumm, I. Halow, S. M. Baily, K. L. Churney, and R. L. Nuttal, "The NBS Tables of Chemical Thermodynamic Properties," J. Phys. Chem. Ref. Data, Vol. 11, suppl. 2 (1982).

[32] V. H. Dibeler and F. L. Mohler, "Dissociation of SF_6, CF_4, and SiF_4 by Electron Impact," J. Res. Nat. Bur. Stand., Vol. 40, pp. 25-29 (1948).

[33] F. Seel, "The Isomers of disulfurdifluoride," Chemia, Vol. 22, pp. 79-83 (1968); F. Seel, E. Heinrich, W. Gombler, and R. Budenz, "Sulfurdifluoride," Chimia, Vol. 23, pp. 73-74 (1969).

[34] R. L. Wilkins, "Thermodynamics of SF_6 and Its Decomposition and Oxidation Products," J. Chem. Phys., Vol. 51, pp. 853-854 (1969).

[35] K. P. Brand and J. Kopainsky, "Particle Densities in a Decaying SF_6 Plasma," Appl. Phys., Vol. 16, pp. 425-432 (1978).

[36] J. F. Bott and T. A. Jacobs, "Shock-Tube Studies of Sulfur Hexafluoride," J. Chem. Phys., Vol. 50, pp. 3850-3855 (1969).

[37] I. Sauers, H. W. Ellis, L. C. Frees, and L. G. Christophorou, "Studies of Spark Decomposition Products of SF_6 and SF_6/Perfluorocarbon Mixtures," Gaseous Dielectrics III (L. G. Christophorou, ed.) Pergamon Press, New York (1982) pp. 387-401; "Detection of SF_4 in Sparked SF_6," IEEE Trans. Elec. Insul., Vol. EI-17, pp. 284-286 (1982).

[38] D. C. Frost, S. T. Lee, C. A. McDowell, and N. P. C. Westwood, "A Versatile, Fast Pumping Ultraviolet Photoelectron Spectrometer for the Study of Transient and Unstable Species," J. Elec. Spec. and Rel. Phenomena, Vol. 12, pp. 95-109 (1977).

[39] The enthalpies of reaction listed apply only at 298 K and in some cases are only approximate due to possible large uncertainties in the heats of formation of species like SF_2, SF_3, SOF_2, and SOF_4 (J. H. Herron, National Bureau of Standards, private communication). The values given were derived from several sources including Ref's 27, 28, and JANAF Thermochemical Tables, J. Phys. Chem. Ref. Data, Vol. 7 (1978) pp. 917; Vol. 3, pp. 387 (1974).

[40] B. Siegel and P. Breisacher, "Oxidation of Sulfur Hexafluoride," J. inorg. nucl. Chem; Vol. 31, pp. 675-683 (1969).

[41] K. L. Wray and E. V. Feldman, "The Pyrolysis and Subsequent Oxidation of SF_6," Proc. 14th Int'l. Symp. on Combust., pp. 229-238 (1972).

[42] L. C. Frees, I. Sauers, H. W. Ellis, and L. G. Christophorou, "Positive Ions in Spark Breakdown of SF_6," J. Phys. D: Appl. Phys., Vol. 14, pp. 1629-1642 (1981).

[43] A. C. Gonzalez and H. J. Schumacher, "The Kinetics of Thermal Reaction between Sulfurtetrafluoride and Flourine in the Presence of Oxygen," Zeit. Phys. Chem. Vol. 127 (1981) pp. 167-177; J. Czarnowski and H. J. Schumacher, "The Kinetics and the Mechanism of the Thermal Decomposition of Bis-Pentafluorosulfurtrioxide (SF_5OOOSF_5)," Int. J. Chem. Kinetics, Vol. 11 (1979) pp. 613-619.

[44] A. M. Velichko, I. O. Leipunskii, A. K. Lyubimova, A. A. Nadeikin, A. I. Nikitin, and V. L. Tal'roze, "Role of Heterogeneous Processes in the Formation of Oxygenated Products During the Multiphoton Dissociation of SF_6 by CO_2 Laser Emission," High Energy Chem., Vol. 17 (1983) pp. 124-127.

[45] R. J. Van Brunt and D. Leep, "Characterization of Point-Plane Corona Pulses in SF_6," J. Appl. Phys., Vol. 52 (1981) pp. 6588-6600.

[46] J. W. Gallagher, E. C. Beaty, J. Dutton, and L. C. Pitchford, "An Annotated Compilation and Appraisal of Electron Swarm Data in Electronegative Gases," J. Phys. Chem. Ref. Data, Vol. 12 (1983) pp. 109-152.

[47] J. P. Novak and M. F. Frechette, "Transport Coefficients of SF_6 and SF_6/N_2 Mixtures from Revised Data," J. Appl. Phys., Vol. 55 (1984) pp. 107-119.

[48] J. Dutton, "A Survey of Electron Swarm Data," J. Phys. Chem. Ref. Data, Vol. 4 (1975) pp. 577-856.

[49] R. J. Van Brunt and M. Misakian, "Mechanisms for Inception of DC and 60-Hz Ac Corona in SF_6," IEEE Trans. on Elec. Insul., Vol. EI-17 (1982) pp. 106-120.

[50] A. V. Oppenheim and A. S. Willsky, Signals and Systems, Prentice-Hall, 1983.

[51] Tikhonov & Arsenin, Solutions of Ill-Posed Problems, Winston, (1977)

[52] O'Leary & Rust, Confidence Internal Estimates for Ill-Posed Problems with Inequality Constraints, to appear in SIAM J. for Scientific and Statistical Computing.

[53] Hestenes & Stiefel, "Methods of Conjugate Gradients for Solving Linear Systems", J. Res. Nat. Bur. Standards, Section B, 49, 1952, pp. 409-436.

U.S. DEPT. OF COMM. BIBLIOGRAPHIC DATA SHEET (See instructions)	1. PUBLICATION OR REPORT NO. NBSIR 85-3112	2. Performing Organ. Report No.	3. Publication Date February 1985

4. TITLE AND SUBTITLE

Development of Power System Measurements --
Quarterly Report April 1, 1984 to June 30, 1984

5. AUTHOR(S)

R. E. Hebner, Jr.

6. PERFORMING ORGANIZATION (If joint or other than NBS, see instructions) NATIONAL BUREAU OF STANDARDS DEPARTMENT OF COMMERCE WASHINGTON, D.C. 20234	7. Contract/Grant No.
	8. Type of Report & Period Covered

9. SPONSORING ORGANIZATION NAME AND COMPLETE ADDRESS (Street, City, State, ZIP)

Department of Energy
Division of Electric Energy Systems
1000 Independence Avenue, SW
Washington, DC 20585

10. SUPPLEMENTARY NOTES

☐ Document describes a computer program; SF-185, FIPS Software Summary, is attached.

11. ABSTRACT (A 200-word or less factual summary of most significant information. If document includes a significant bibliography or literature survey, mention it here)

This report documents the progress of three technical investigations sponsored by the Department of Energy and performed by or under a grant from the Electrosystems Division, the National Bureau of Standards. The work described covers the period April 1, 1984 to June 30, 1984. This report emphasizes the errors associated with measurements of dc electric fields, the properties of corona in compressed SF_6 gas, and the measurement of voltage pulses on nanosecond time scales.

12. KEY WORDS (Six to twelve entries; alphabetical order; capitalize only proper names; and separate key words by semicolons)

deconvolution; electric fields; gaseous insulation; partial discharges; pulsed voltage measurement; SF_6; solid insulation

13. AVAILABILITY	14. NO. OF PRINTED PAGES
☒ Unlimited	
☐ For Official Distribution. Do Not Release to NTIS	39
☐ Order From Superintendent of Documents, U.S. Government Printing Office, Washington, D.C. 20402.	15. Price
☒ Order From National Technical Information Service (NTIS), Springfield, VA. 22161	$8.50